Plasma 2
Lecture 20:
Interchange, Ballooning, and Kinks

APPH E6102y
Columbia University

Low-Frequency (Electro-)Magnetic Response in a Strongly Magnetized Plasma

- ALFVEN WAVES (REVIEW) (From *Lecture-9*)
- MAGNETIC INDUCTIONS (FARADAY'S LAW)
- WHEN $E_{\parallel} = 0$ ∴ THE IDEAL MHD CONDITION

  AND WHEN NOT $E_{\parallel} \neq 0$

  DRIFT WAVES $\tilde{E}_{\parallel} = -i k_{\parallel} \tilde{\phi}$ $\quad k^2 \rho^2 \sim 1$ & $k_{\parallel} v_A \gg \omega$ (SHORT WAVELENGTH; LOW FREQ)

  MHD WAVES $\tilde{E}_{\parallel} = 0$ $\quad k_{\parallel} \to 0$ OR $k^2 \rho^2 \ll 1$ (INTERCHANGE FLUTE-LIKE; LONG WAVELENGTH)

Parallel Electric Field

$$E_\parallel = -i k_\parallel \tilde{\Phi} + i \omega \tilde{A}_\parallel$$

$$= i k_\parallel \tilde{\Phi} \left[\frac{k^2 \rho^2 k_\parallel^2 V_A^2}{\omega(\omega - k v_D^*) - k^2 \rho^2 k_\parallel^2 V_A^2} \right]$$

(wow!!)

WHEN $k^2 \rho^2 k_\parallel^2 V_A^2 \gg \omega^2$

$$E_\parallel \cong -i k_\parallel \tilde{\Phi}$$

← USUAL DRIFT WAVE LIMIT

WHEN $k_\parallel \to 0$ AND/OR $k^2 \rho^2 \ll 1$

$$\tilde{E}_\parallel = 0$$

← USUAL MHD LIMIT

Density-Potential Relationship

MAGNETIC FLUCTUATION POTENTIAL:

$$\left(\frac{e\tilde{A}}{T}\right) = \frac{k_\parallel (\omega - k_y v_D^*)}{\omega(\omega - k_y v_D^*) - k^2\rho^2 k_\parallel^2 v_A^2}\left(\frac{e\tilde{\Phi}}{T}\right)$$

CONTINUITY:

$$\frac{\tilde{n}}{n_0} = \frac{k_y v_D^*}{\omega}\left(\frac{e\tilde{\Phi}}{T}\right) - k^2\rho^2 v_A^2 \frac{k_\parallel}{\omega}\left(\frac{e\tilde{A}_\parallel}{T}\right)$$

ELIMINATING $\tilde{A}_\parallel$ ...

$$\frac{\tilde{n}}{n_0} = \left(\frac{e\tilde{\Phi}}{T}\right)\left[1 - \frac{(\omega - k_y v_D^*)^2}{\omega(\omega - k_y v_D^*) - k^2\rho^2 k_\parallel^2 v_A^2}\right]$$

DRIFT LIMIT

$k_\parallel v_A \gg \omega \quad k_y\rho \sim 1$

$$\frac{\delta n}{n} = \frac{e\tilde{\Phi}}{T}$$

MHD LIMIT

$k^2\rho^2 \ll 1 \quad (\text{or } k_\parallel \to 0)$

$$\frac{\delta n}{n} = \left(\frac{k_y v_D^*}{\omega}\right)\left(\frac{e\tilde{\Phi}}{T}\right)$$

PURE E×B CONVECTION WHEN PARALLEL MOTION IS IGNORED

Low-Frequency MHD Modes

- INTERCHANGE MODES $k_{\parallel} = 0$ (PRESSURE DRIVEN)
- KINK MODES $E_{\parallel} = 0$ BUT ELECTROMAGNETIC $\tilde{A}_{\parallel} \neq 0$ (CURRENT-GRADIENT DRIVEN)
- BALLOONING MODES $k_{\parallel} \neq 0$ (PRESSURE DRIVEN)
- { TEARING MODES ($k_{\parallel} = 0$ ONLY ON RATIONAL SURFACE)
  MICRO TEARING MODES (LARGER $k_{\perp}$) } (KINKS DESTABILIZED BY COLLISIONS)

COMMENT: KINK MODES, BALLOONING MODES, TEARING MODES ARE USUALLY DEVELOPED TO LEADING ORDER BY MHD EQUATIONS BUT FULL KINETIC AND TWO-FLUID DYNAMICS ARE NEEDED TO UNDER MHD MODE DYNAMICS SEEN IN EXPERIMENTS.

F-Layer Spread

- Gravitational Rayleigh-Taylor instabilities are well-studied examples of turbulent interchange dynamics.
- Notes: (i) Large scales, (ii) Rayleigh-Taylor regime & Drift-wave regime
- Refs:
  - Kelly, *The Earth's Ionosphere,* (Academic, 1989).
  - Kelly, Franz, Prasad, *J. Geophys. Res.*, **107,** 1432 (2002).

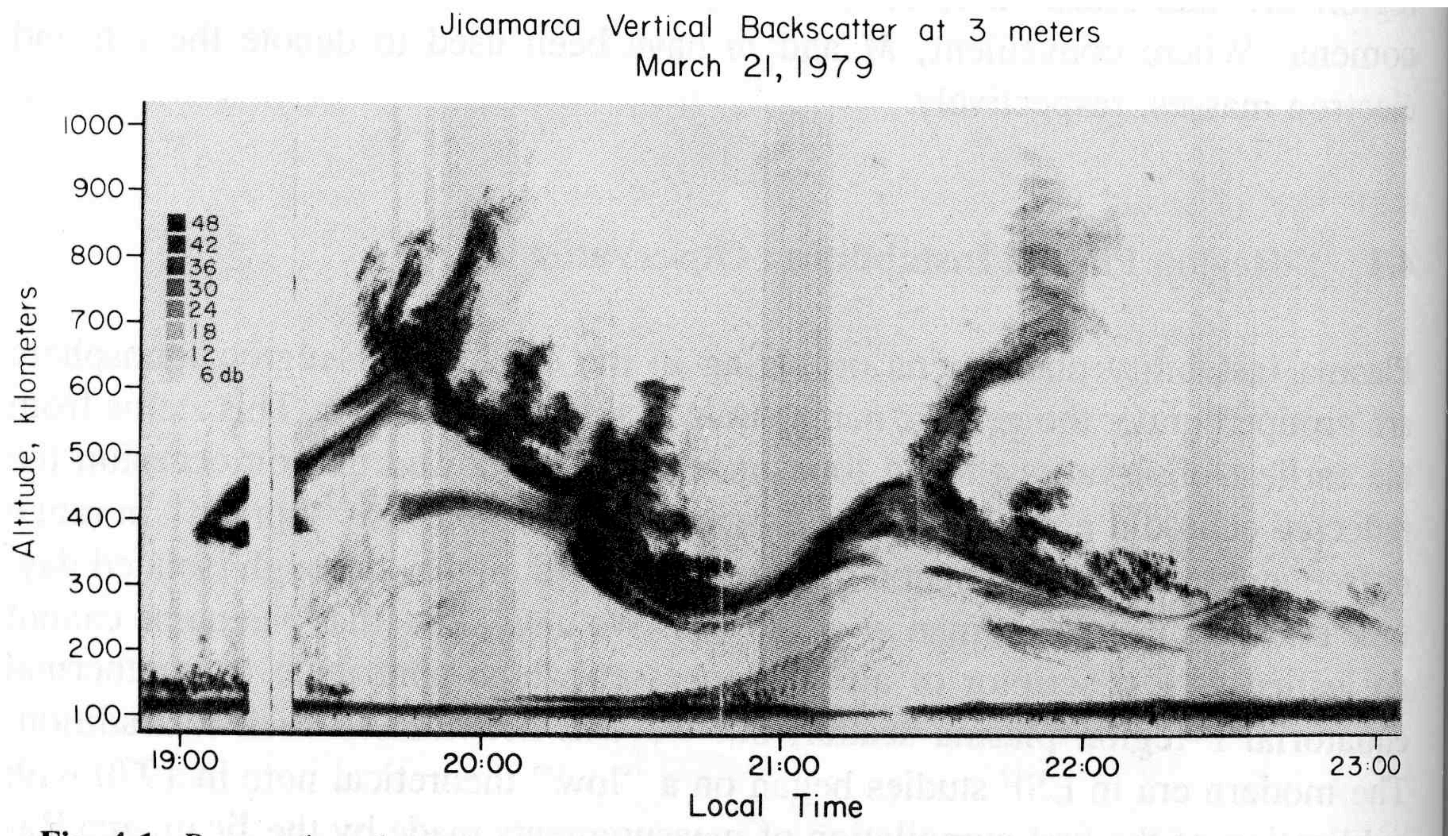

Fig. 4.1. Range–time–intensity map displaying the backscatter power at 3-m wavelengths measured at Jicamarca, Peru. The gray scale is decibels above the thermal noise level. [After Kelley *et al.* (1981). Reproduced with permission of the American Geophysical Union.]

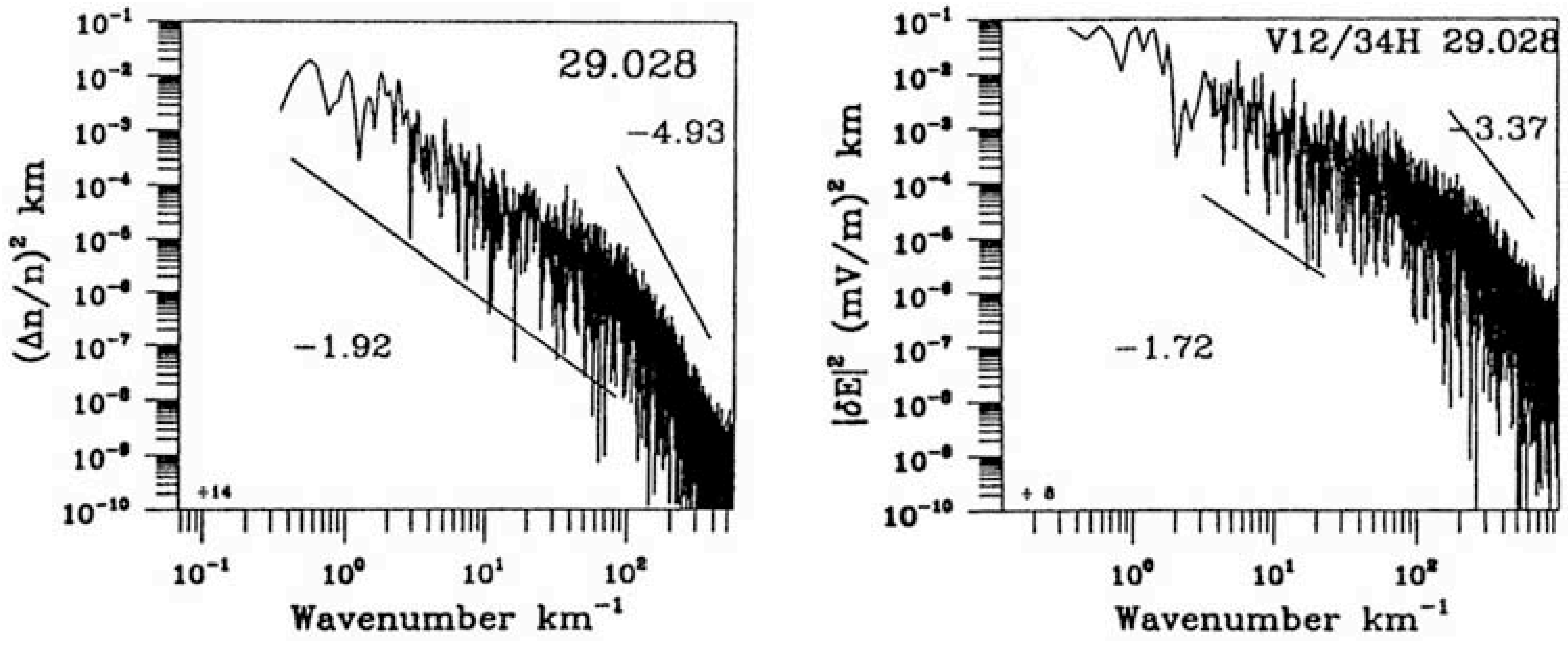

Figure 2. Electron density and electric field spectra measured during the downleg of 29.028 on 30 July 1990. The altitude range covers ∼20 km near 350 km altitude.

Observation of Ballooning Modes in High-Temperature Tokamak Plasmas

Y. Nagayama,[a] S. A. Sabbagh,[b],[c] J. Manickam, E. D. Fredrickson, M. Bell, R. V. Budny, A. Cavallo,[d] A. C. Janos, M. E. Mauel,[b] K. M. McGuire, G. A. Navratil,[b] G. Taylor, and M. Yamada
Plasma Physics Laboratory, Princeton University, P.O. Box 451, Princeton, New Jersey 08543
(Received 8 June 1992)

The beta-degradation phase of a high-β_p plasma in the TFTR tokamak is analyzed with x-ray and electron cyclotron emission imaging techniques. Medium-n (toroidal mode number) instabilities with ballooning characteristics are observed near and within the $q=1.5$ surface during a slow degradation in the plasma β and precede a sudden partial collapse in the central plasma pressure. This is the first reported observation of a ballooning instability in the interior of a large, collisionless tokamak plasma.

Tokamak Ballooning Modes

VOLUME 69, NUMBER 16 PHYSICAL REVIEW LETTERS 19 OCTOBER 1992

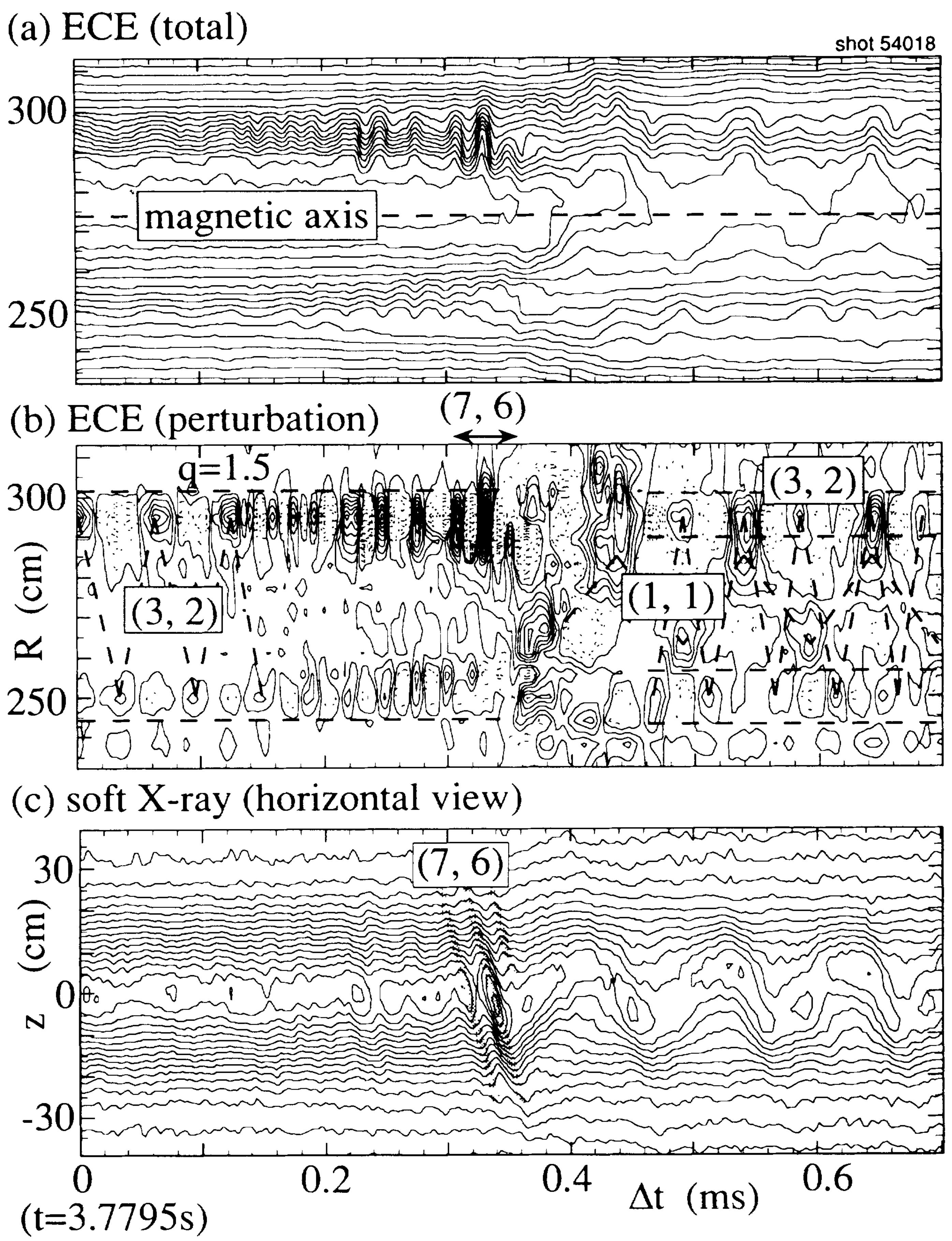

FIG. 2. Contour plots of the time evolution of the ECE profile in shot 54018: (a) Electron temperature profile (the contour step size is 300 eV); (b) perturbation of ECE signal; (c) chord-integrated soft-x-ray emission profile (horizontal view).

3 cm. The soft x rays are detected with a vertical viewing camera (twenty detectors) and a horizontal viewing cam-

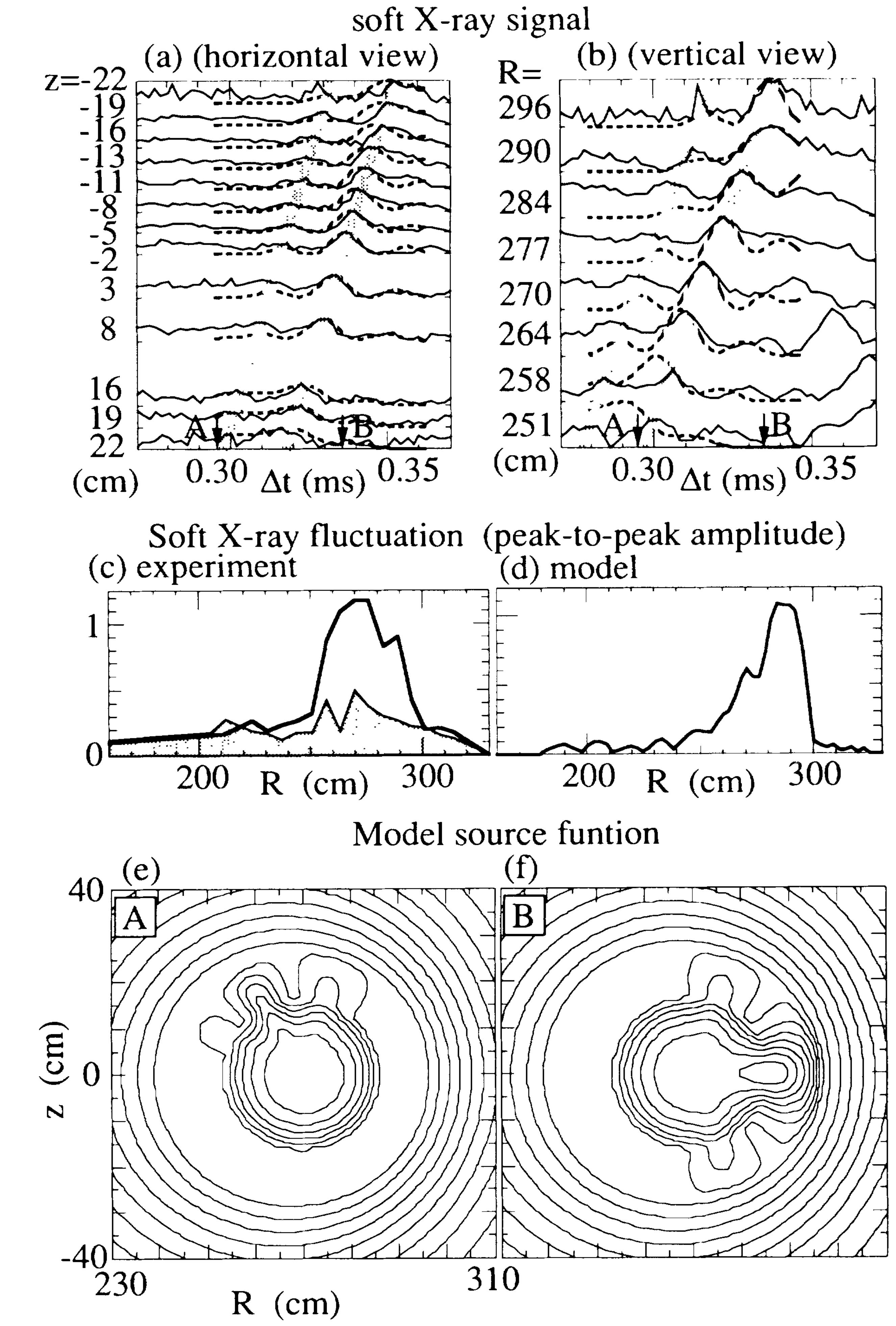

FIG. 3. Comparison of observed soft-x-ray signals and the signals simulated by the model source function: (a) The observed soft-x-ray signals from the horizontal camera, and the simulated wave forms from the horizontal camera by the $(m,n)=(7,6)$ model, where the solid line represents experimental signal and the dotted line represents model simulation; (b) the observed soft-x-ray signals from the vertical camera, and

Large-Larmor-Radius Interchange Instability

B. H. Ripin, E. A. McLean, C. K. Manka, C. Pawley,[a] J. A. Stamper, T. A. Peyser,[a] A. N. Mostovych, J. Grun, A. B. Hassam,[a] and J. Huba
Naval Research Laboratory, Washington, D.C. 20375
(Received 15 June 1987)

We observe linear and nonlinear features of a strong plasma–magnetic-field interchange Rayleigh-Taylor instability in the limit of large ion Larmor radius. The instability undergoes rapid linear growth culminating in free-streaming flute tips.

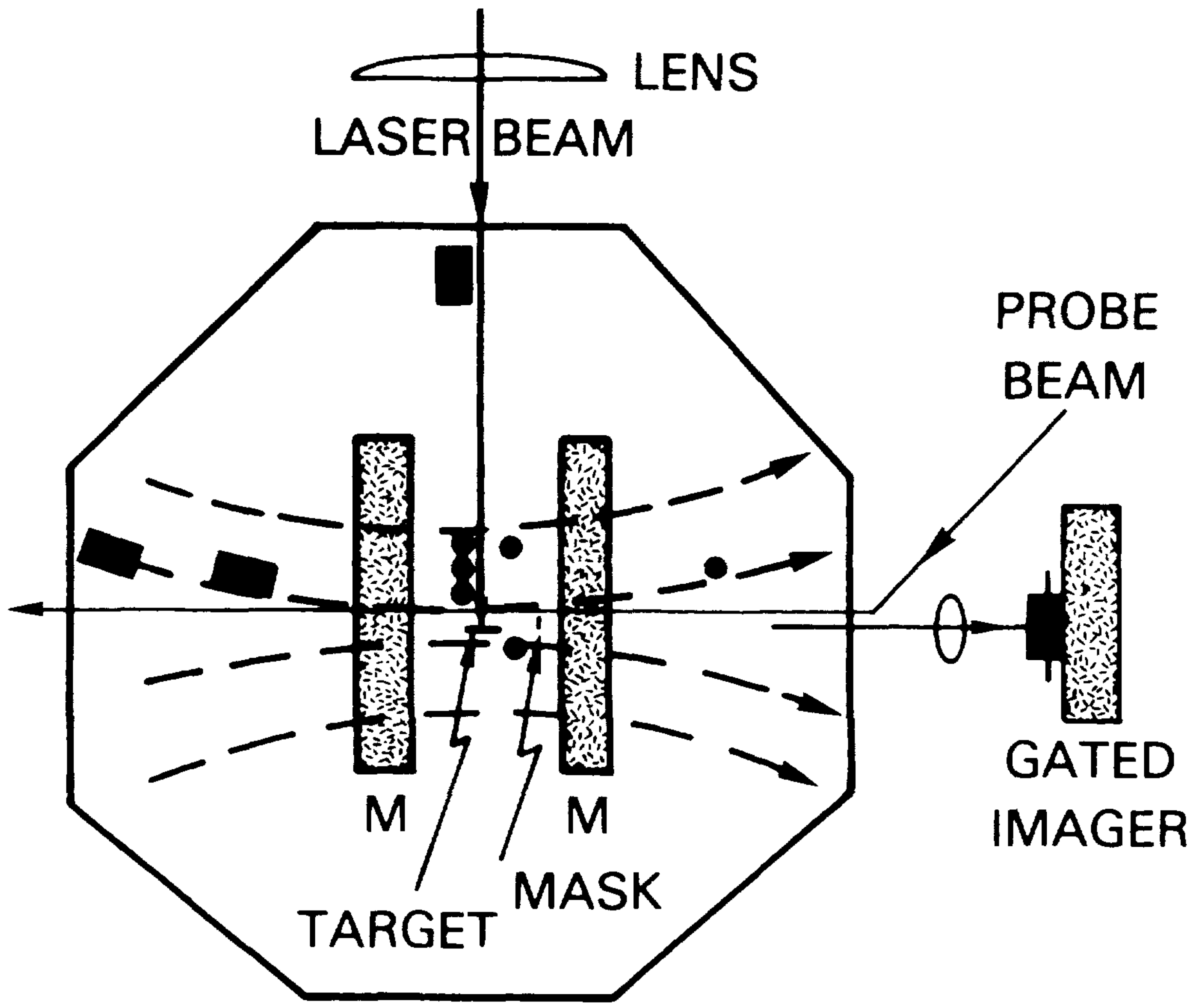

FIG. 1. Experimental arrangement for instability experiments. A schematic of the equipment is shown; ion detectors are denoted by rectangles and magnetic probes by circles.

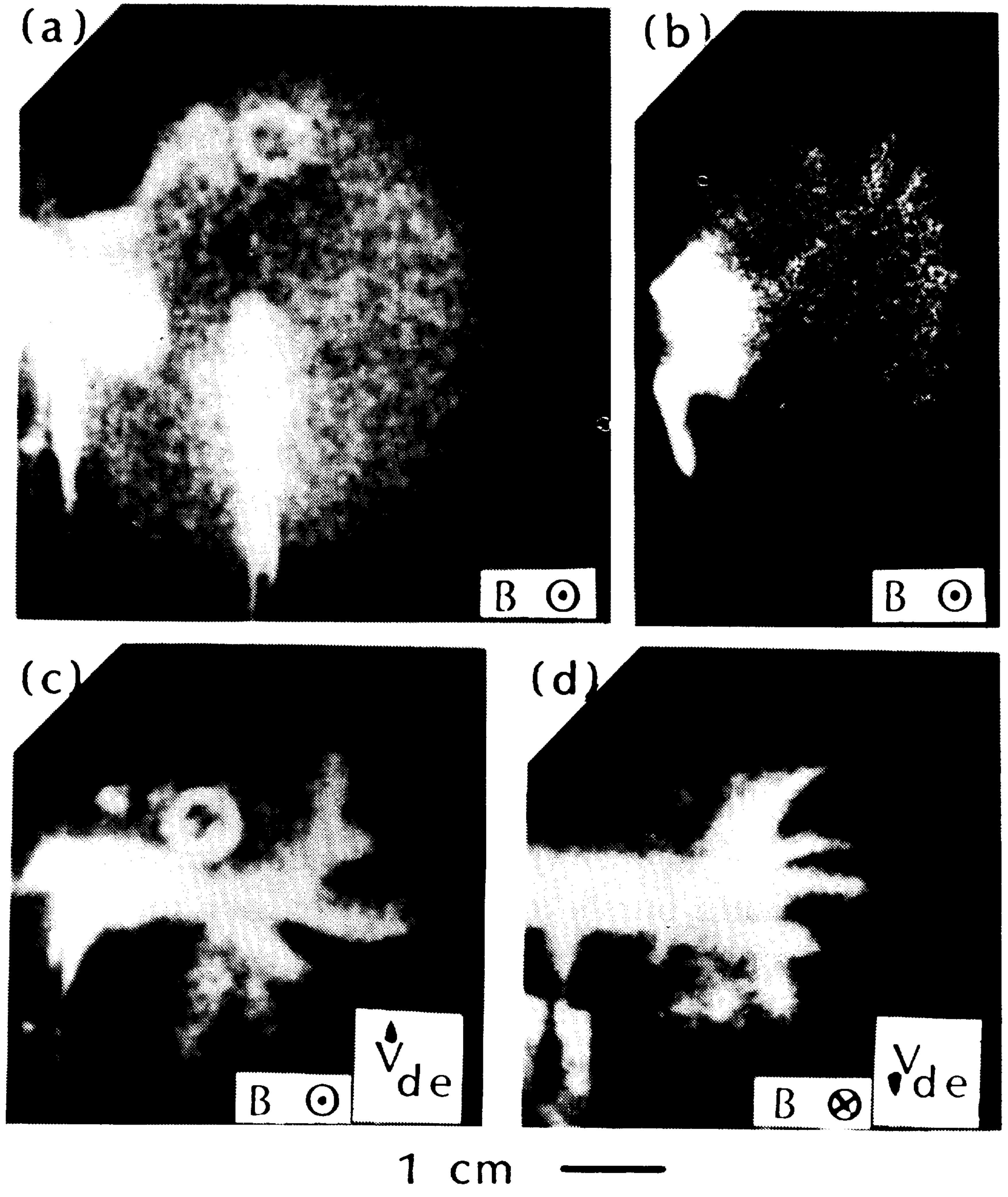

FIG. 3. Examples of the instability development. (a) 0.1-T case observed at time 115 ns. (b) Example of density clumps in the early time phase development with $B = 1.0$ T at time 59 ns. (c) Example of curved spike structure with 1.0-T field (field points out of paper) at 115 ns. (d) Same as (c) except field points into paper and $t = 100$ ns; note reversal of curvature sense. $E_1 = 25-30$ J and $P < 0.1$ mTorr for these shots.

474 J. LEMAIRE and L. KOWALKOWSKI

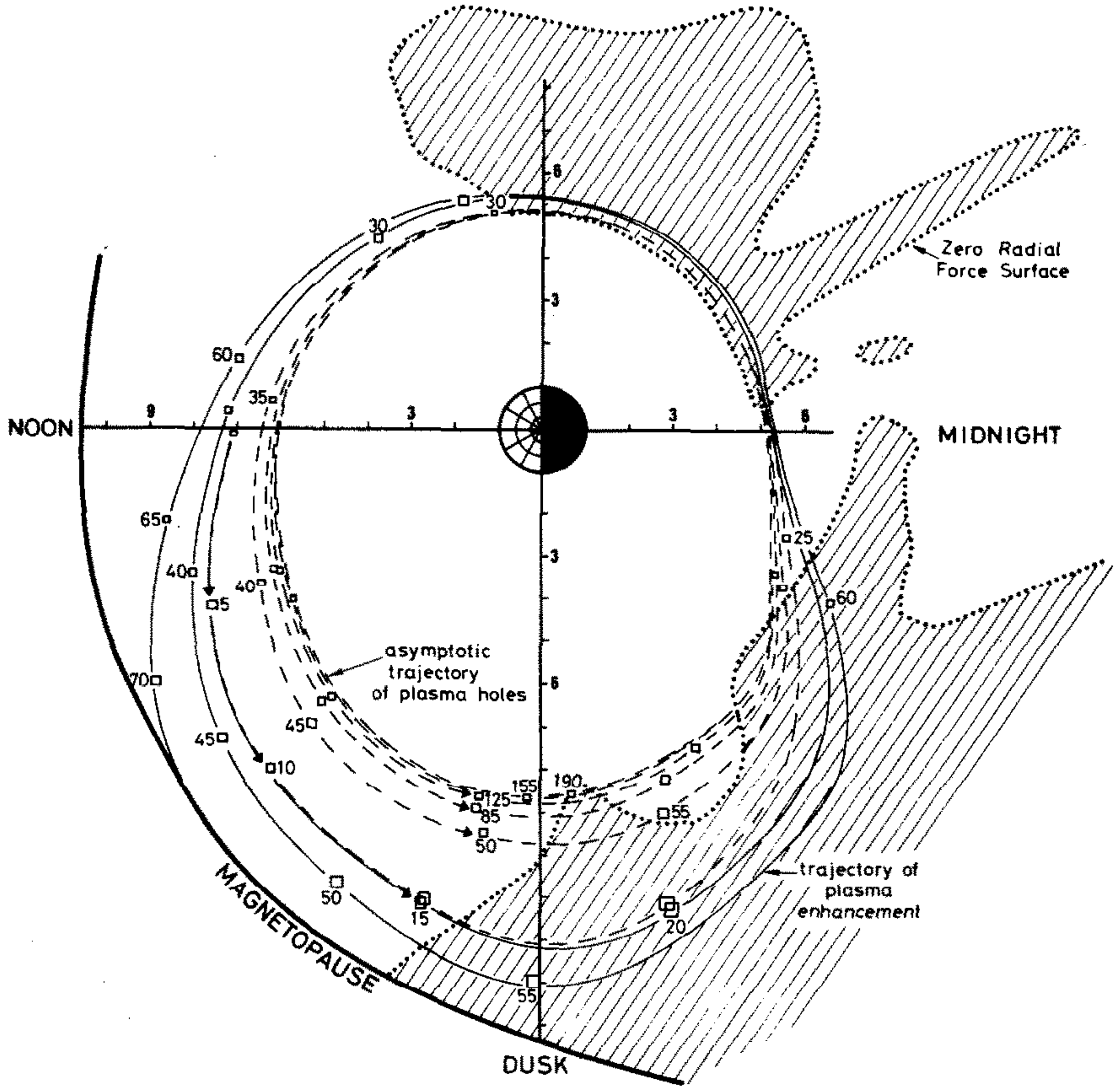

FIG. 6. EQUATORIAL DRIFT PATH OF A 20 % PLASMA DENSITY ENHANCEMENT (SOLID LINE) AND OF A PLASMA HOLE (DASHED LINE) RELEASED AT $R = 7\ R_E$. OTHERWISE THE CONDITIONS AND NOTATIONS ARE THE SAME AS IN FIG. 5.

Note that the plasma density enhancement now drifts outwards. Under the dominating action of the centrifugal force whose radial component exceeds the gravitational force everywhere in the shaded area beyond the Zero-Radial-Force Surface. The plasma hole spirals in the opposite direction toward the same asymptotic trajectory as the plasma hole in Fig. 5. This asymptotic trajectory of all plasma holes determines the position of the equatorial plasmapause.

Plasmapause

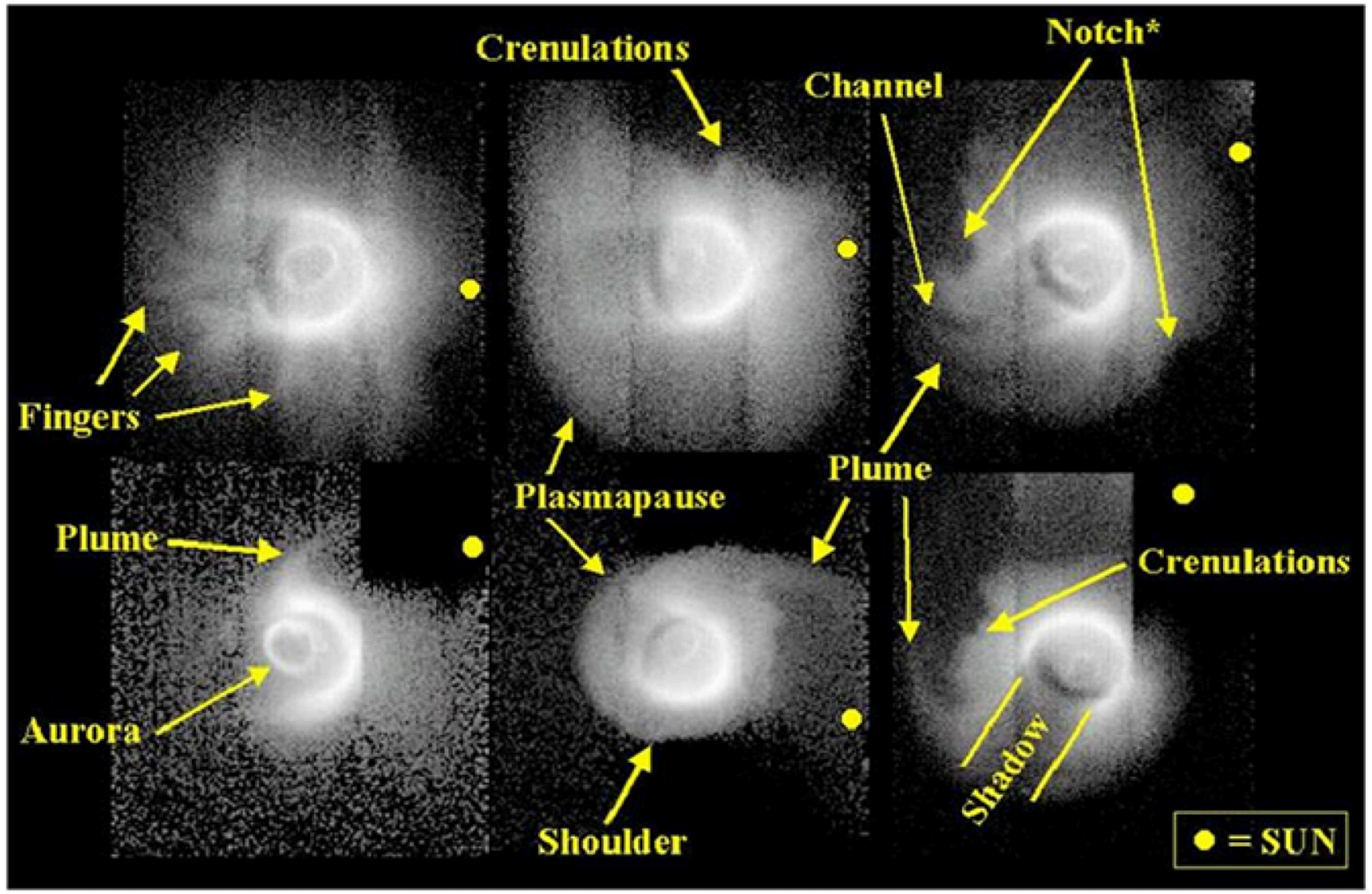

Fig. 1 Structures observed by the EUV instrument onboard IMAGE and new morphological nomenclature: examples of shoulders, plumes, fingers, channels, crenulations and notches. The direction to the Sun is shown as a *yellow dot* for each image. (From http://image.gsfc.nasa.gov/poetry/discoveries/N47big.jpg)

Io Plasma Torus

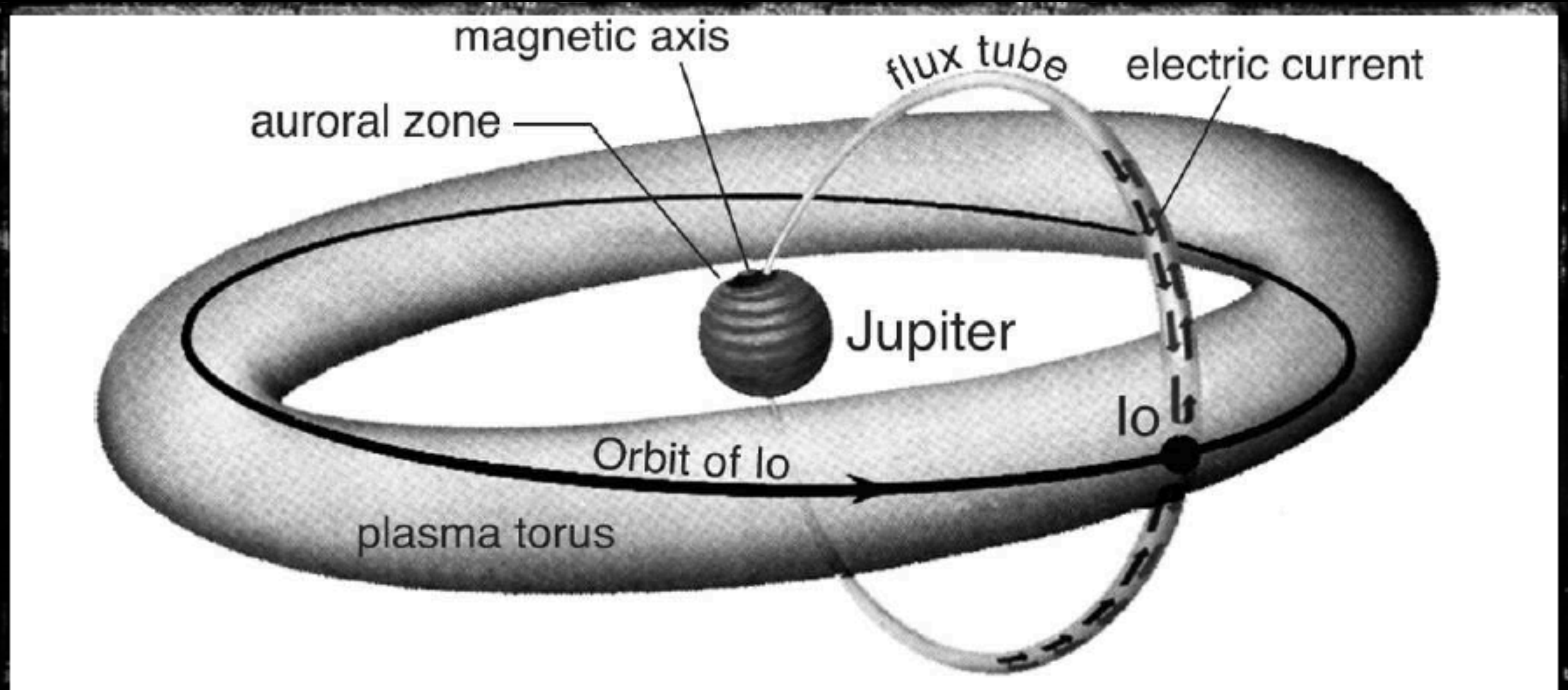

Figure 22.1. Sketch of the Io plasma torus and the general geometrical setup, after Audouze et al. 1988.

Magnetospheric Dynamo:
100 TW Auroral Power
Regulates Interchange Motion

Hill and Vasyliūnas, "Jovian auroral signature of Io's corotational wake," JGR, 107, 1464 (2002).

Hubble (Dec 9, 2000)

Io Plasma Torus

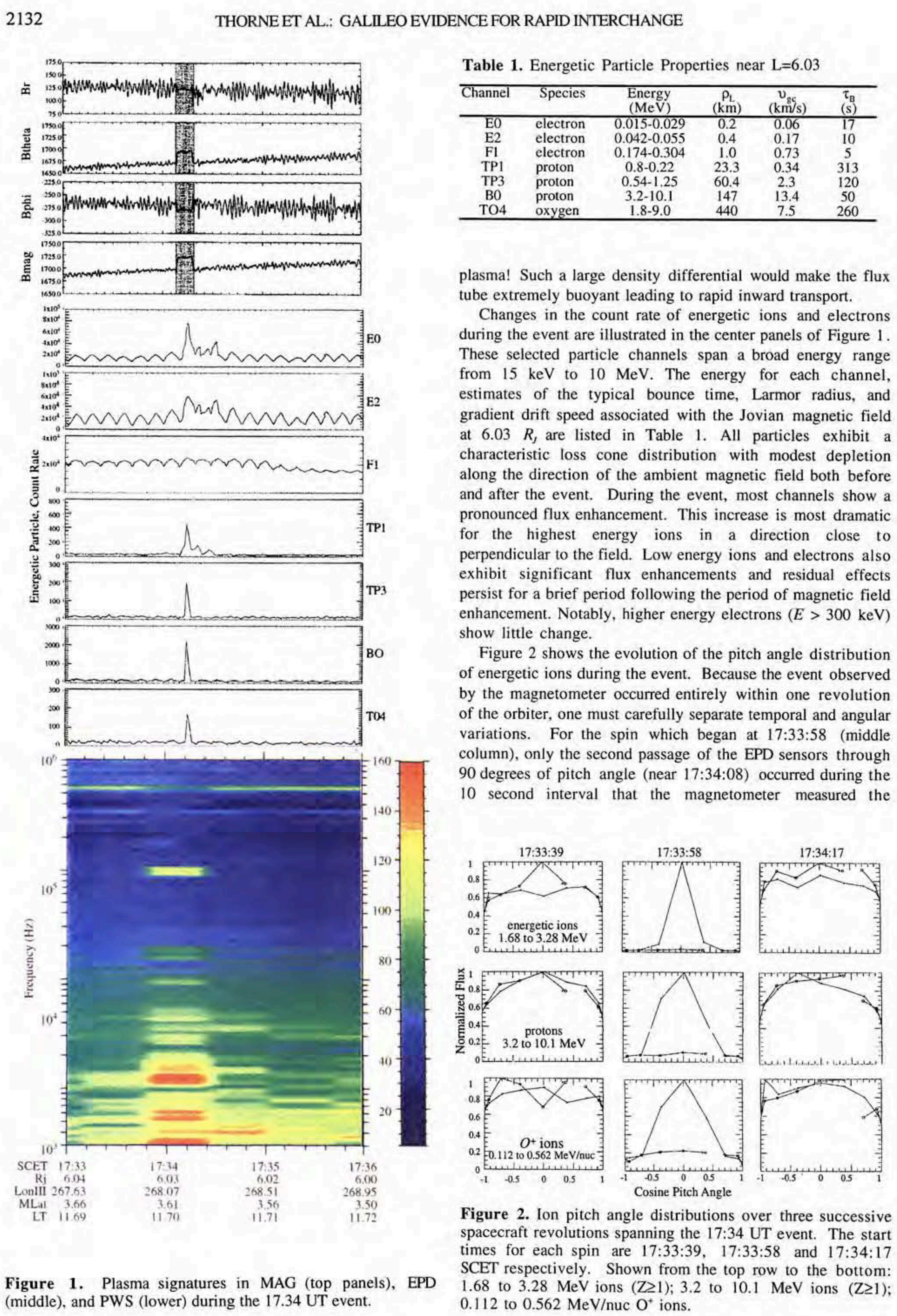

Table 1. Energetic Particle Properties near L=6.03

Channel	Species	Energy (MeV)	ρ_L (km)	v_{gc} (km/s)	τ_B (s)
E0	electron	0.015-0.029	0.2	0.06	17
E2	electron	0.042-0.055	0.4	0.17	10
F1	electron	0.174-0.304	1.0	0.73	5
TP1	proton	0.8-0.22	23.3	0.34	313
TP3	proton	0.54-1.25	60.4	2.3	120
B0	proton	3.2-10.1	147	13.4	50
TO4	oxygen	1.8-9.0	440	7.5	260

plasma! Such a large density differential would make the flux tube extremely buoyant leading to rapid inward transport.

Changes in the count rate of energetic ions and electrons during the event are illustrated in the center panels of Figure 1. These selected particle channels span a broad energy range from 15 keV to 10 MeV. The energy for each channel, estimates of the typical bounce time, Larmor radius, and gradient drift speed associated with the Jovian magnetic field at 6.03 R_J are listed in Table 1. All particles exhibit a characteristic loss cone distribution with modest depletion along the direction of the ambient magnetic field both before and after the event. During the event, most channels show a pronounced flux enhancement. This increase is most dramatic for the highest energy ions in a direction close to perpendicular to the field. Low energy ions and electrons also exhibit significant flux enhancements and residual effects persist for a brief period following the period of magnetic field enhancement. Notably, higher energy electrons ($E > 300$ keV) show little change.

Figure 2 shows the evolution of the pitch angle distribution of energetic ions during the event. Because the event observed by the magnetometer occurred entirely within one revolution of the orbiter, one must carefully separate temporal and angular variations. For the spin which began at 17:33:58 (middle column), only the second passage of the EPD sensors through 90 degrees of pitch angle (near 17:34:08) occurred during the 10 second interval that the magnetometer measured the

Figure 1. Plasma signatures in MAG (top panels), EPD (middle), and PWS (lower) during the 17.34 UT event.

Figure 2. Ion pitch angle distributions over three successive spacecraft revolutions spanning the 17:34 UT event. The start times for each spin are 17:33:39, 17:33:58 and 17:34:17 SCET respectively. Shown from the top row to the bottom: 1.68 to 3.28 MeV ions (Z≥1); 3.2 to 10.1 MeV ions (Z≥1); 0.112 to 0.562 MeV/nuc O^+ ions.

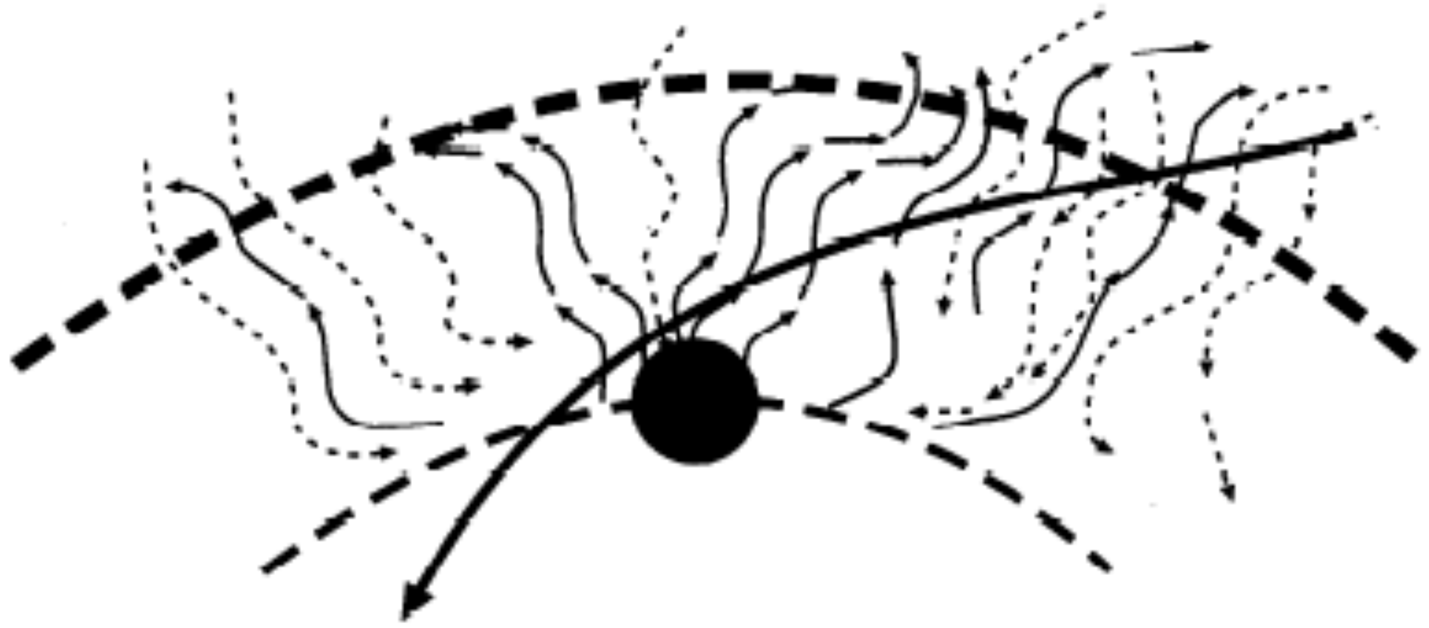

Figure 5. Schematic of the transport envisaged to account for the observations. Dashed arcs are placed at the orbit of Io, and 7 R_J. Meandering curves are not instantaneous streamlines but some average flow paths that would organize our data. Flux tubes moving out (solid curves) have larger plasma content than do those moving in (dashed curves). The azimuthal meanders indicate that random variations in convection fields may produce fluctuations of average azimuthal velocity. The important point is that well away from Io, the inward and outward flows balance. Along Galileo's orbit in the immediate vicinity of Io (filled circle) where mass loading is concentrated, the flow is predominantly outward. Somewhere else the inward flow dominates. The Galileo trajectory inbound to Jupiter (solid curve), crosses inward and outward moving flux tubes near 7 R_J but principally outward moving flux tubes in the near-Io region.

Kink Instabilities: The Most Dangerous Instability for Current-Carrying Plasma

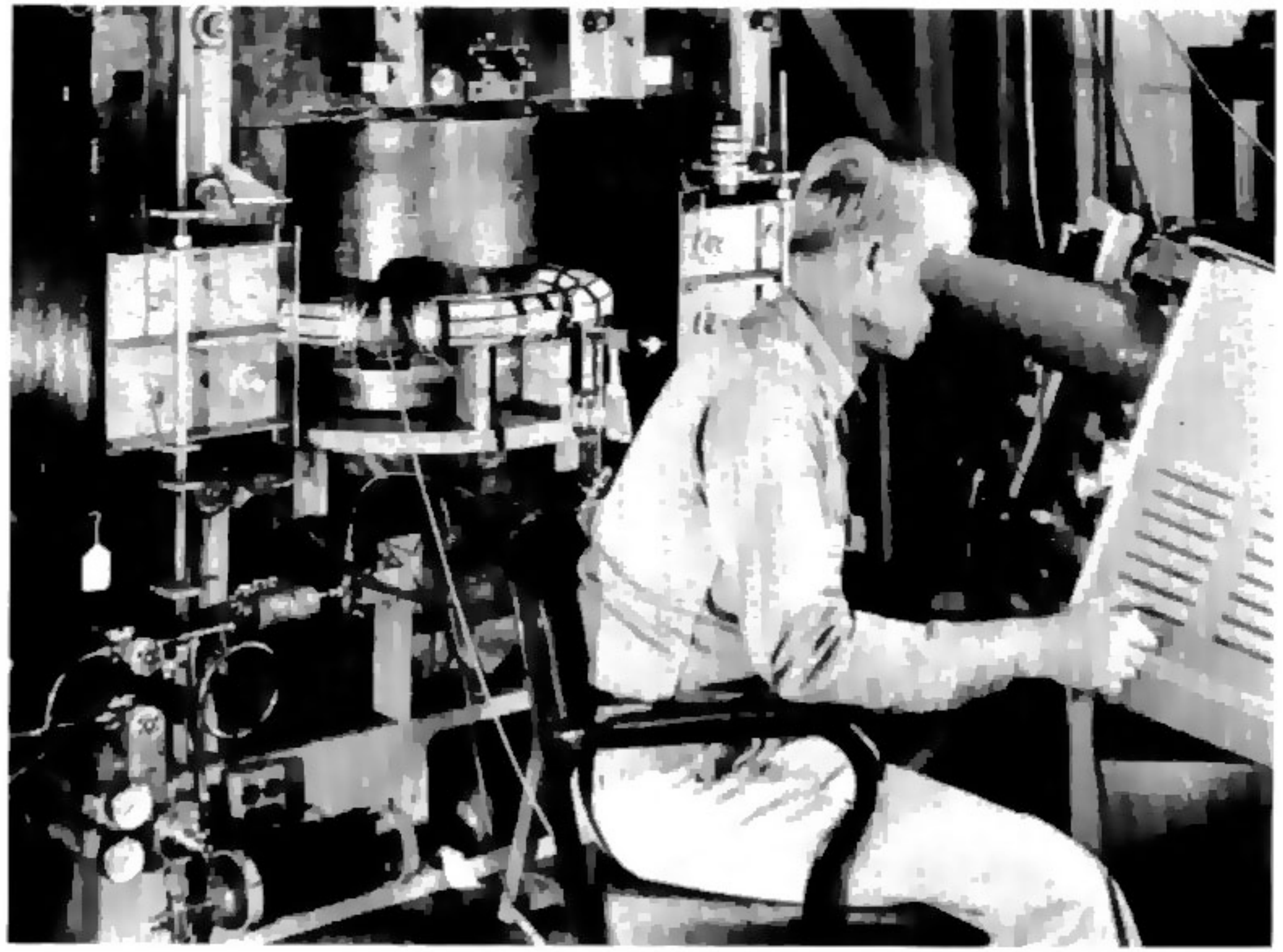

The Perhapsatron, which was built in 1952-53, was the first Z-pinch device at Los Alamos. The toroidal discharge tube surrounds the central core of an iron transformer.

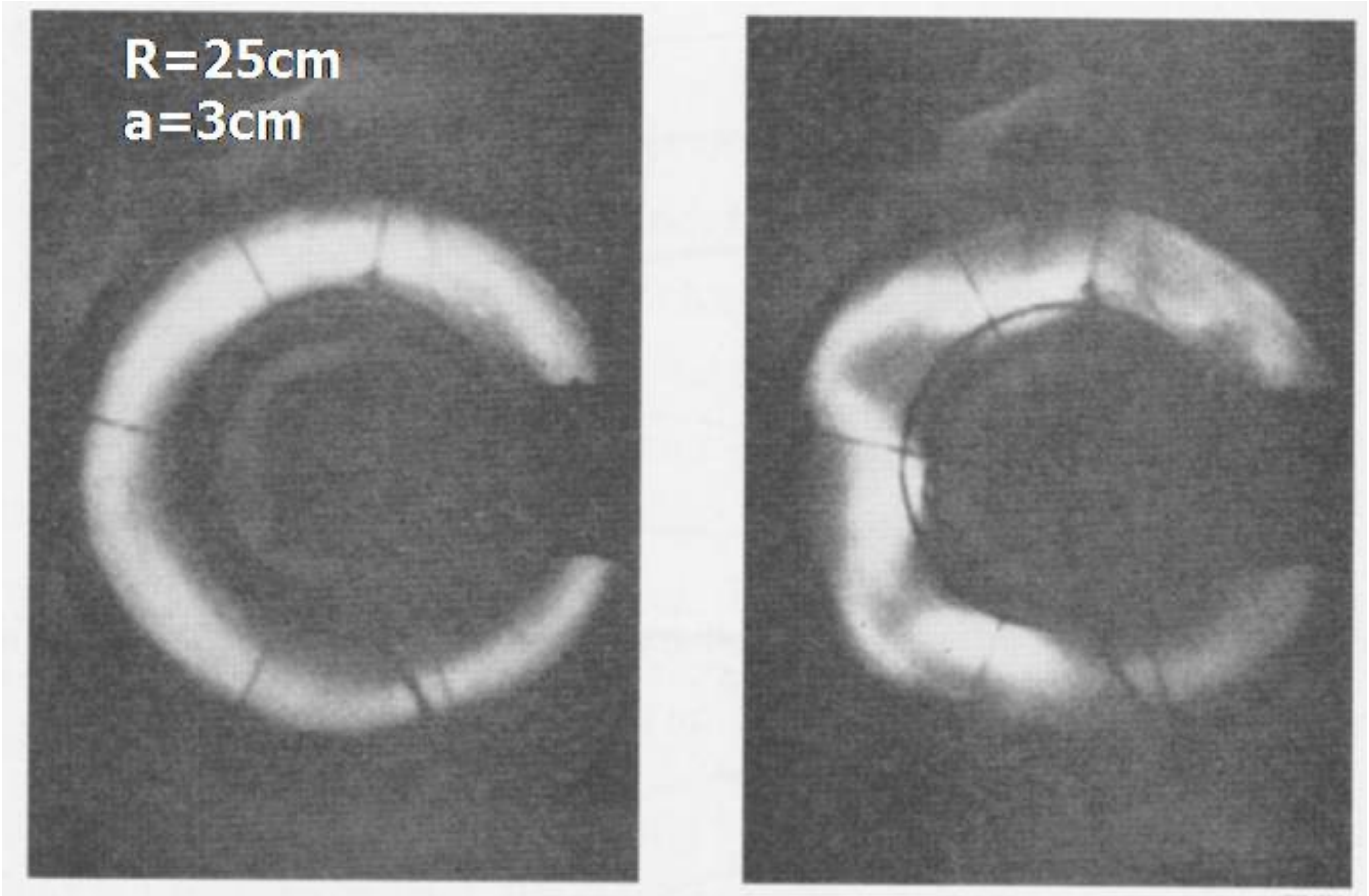

Toroidal “z-pinch”

Interchange Mode Gravity (& Effective Gravity)

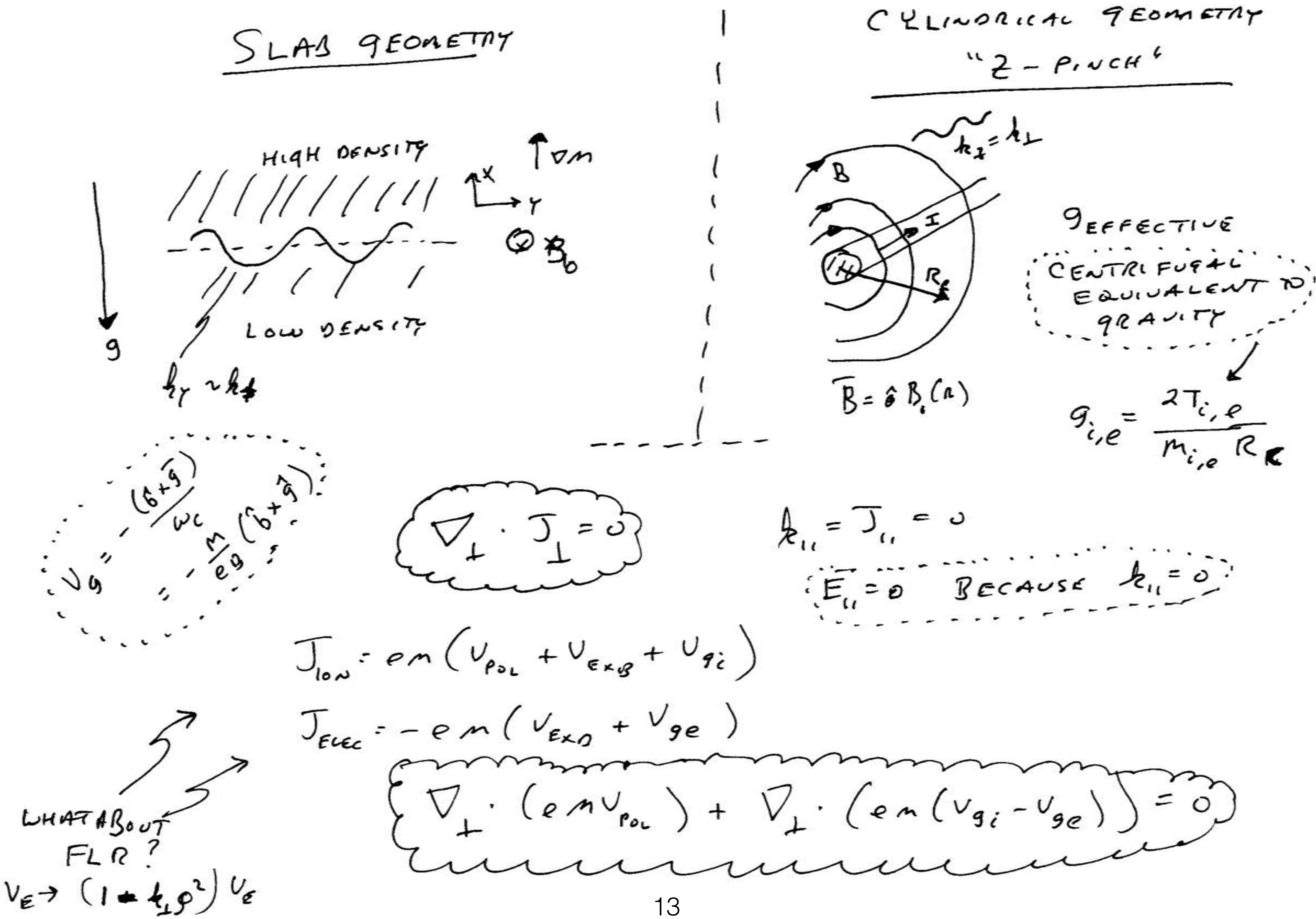

Dispersion Relation: Gravitational Interchange in Slab Geometry

$$V_{pol} = \frac{eM_i}{B_0^2}\frac{d\tilde{E}}{dt} = -\frac{eM_i}{B_0^2}\left(\frac{\partial}{\partial t} + V_{gi}\cdot\nabla\right)\nabla_\perp\tilde{\Phi}$$

$$V_{gi} - V_{ge} = \hat{y}\,\frac{M_i}{eB_0}\left(g + \frac{m_e}{m_i}g\right)$$

WHAT IS KINETIC BALLOONING MODE? LANDAU DAMPING

CHARGE NEUTRALITY

$$\nabla\cdot J_\perp = 0$$

$$\nabla_\perp\cdot\left(e n \bar{V}_{pol}\right) + e\left(V_{gi} - V_{ge}\right)\hat{y}\cdot\nabla\tilde{n} = 0$$

$$\frac{jM_i}{B^2}\nabla_\perp\cdot\left(\omega - k_y V_{gi}\right)\nabla_\perp\tilde{\Phi} + j k_y V_{gi}\frac{\tilde{n}}{n_0} = 0$$

$$-\left(\omega - k_y V_{gi}\right)k^2\tilde{\Phi} + k_y V_{gi}\frac{B^2}{m_i}\frac{\tilde{n}}{n_0} = 0$$

CONTINUITY

$$\frac{\partial\tilde{n}}{\partial t} + \nabla\cdot\left(n\bar{V}\right) = 0$$

ELECTRONS

$$\frac{\partial\tilde{n}}{\partial t} + \bar{V}_E\cdot\nabla n_0 = 0$$

$$-j\omega\tilde{n} - n_0\frac{j k_y\tilde{\Phi}\,(n'/n)}{B_0} = 0$$

$$\frac{\tilde{n}}{n_0} = \frac{k_y V_{De}^*}{\omega}\left(\frac{e\tilde{\Phi}}{T_e}\right)$$

WHY?

$$V_{D0} = \frac{T_e}{eB_0}(\ldots$$

$$\omega\left(\omega - k_y V_{gi}\right) = +\left(\frac{n'}{n_0}\right) g\, k_y^2/k^2$$

$\left(\frac{n'}{n_0}g\right) < 0$ UNSTABLE

Gravitational Interchange in Slab Geometry

THIS IS <0 FOR INSTABILITY

$$\omega^2 - \omega k_y v_{gi} - \left(\frac{n'}{n_0} g\right)\frac{k_y^2}{k^2} \approx 0$$

$$\omega = \frac{k_y v_{gi}}{2} \pm \sqrt{\left(\frac{k_y v_{gi}}{2}\right)^2 + \left(\frac{n'}{n_0} g\right)\frac{k_y^2}{k^2}}$$

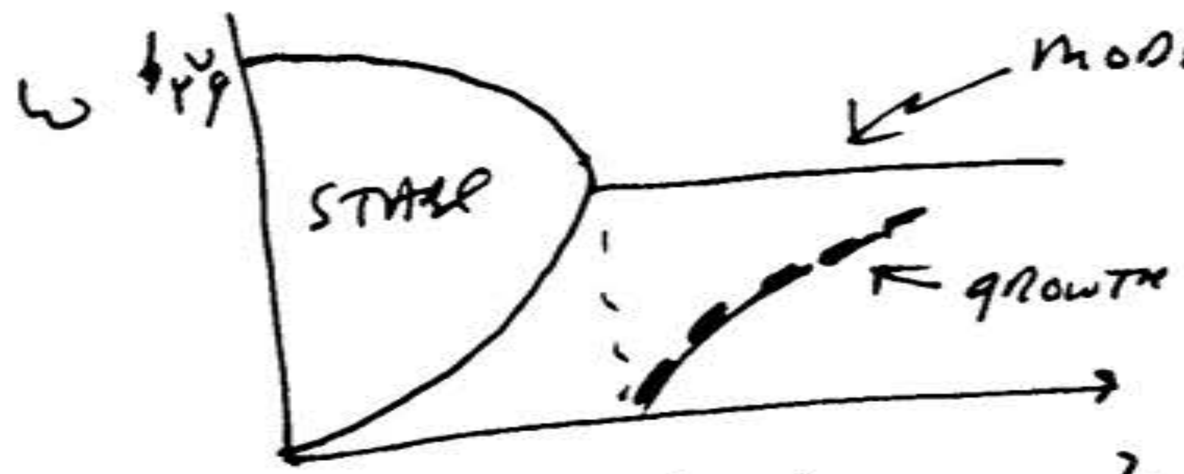

$$\left|\frac{n'}{n_0} g\right| > k^2 \;!!$$

← SHORTER WAVELENGTHS

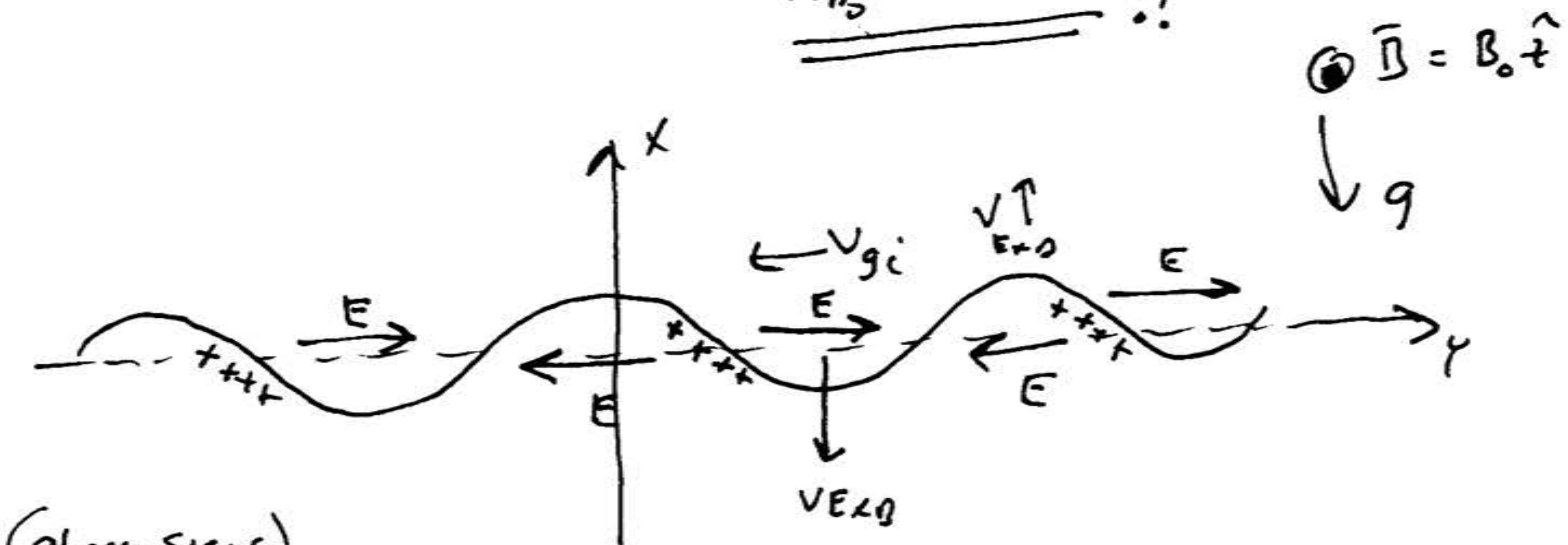

$$v_{gi} = -\frac{m}{eB}\left(\hat{B} \times \vec{g}\right)$$

$$\vec{g} = -\hat{x}\, g$$

(Check signs)

Estimate: Curvature-Driven Interchange ("Cylindrical" Geometry)

GRAVITY → CURVATURE

$V_{DIA}^* \propto \nabla P$

$$\nabla_\perp \cdot en(V_{gi} - V_{ge}) \rightarrow \nabla \cdot (en V_{DIA}^*)$$

g (EFFECTIVE) $= \dfrac{2T}{n R_c}$

$V_g(\text{EFF}) = -\dfrac{m}{eB} g_{\text{EFF}}$

DRIVE: $\left(\dfrac{n'}{n}\right) g \dfrac{k_y^2}{k^2} \rightarrow \left(\dfrac{P'}{P}\right) \dfrac{2(T_e + T_i)}{m_i R_c} \dfrac{k_y^2}{k^2}$

$\underbrace{}$ – (DRIVE)

$$\omega(\omega - k_y V_{\text{DRIFT}}) = -(\text{DRIVE}) \frac{k_y^2}{k^2}$$

$\dfrac{P'}{P} = \dfrac{n'}{n}(1 + \eta)$

$\eta \equiv \dfrac{d \ln T}{d \ln n}$

BOTH ION DENSITY
ION TEMPERATURE
GRADIENTS
COUNT!

THIS ACTUALLY BECOMES ION FLR STABILIZATION

ION FLR:

$k_y V_{\text{DRIFT}} \rightarrow k_y V_{DIA}^*$

$\propto \frac{1}{R_c} \quad \propto \frac{1}{a}$

SHORTER WAVELENGTHS TEND TO BE MOST UNSTABLE WHEN $k_\parallel = 0$

Ballooning Modes

EXAMPLE

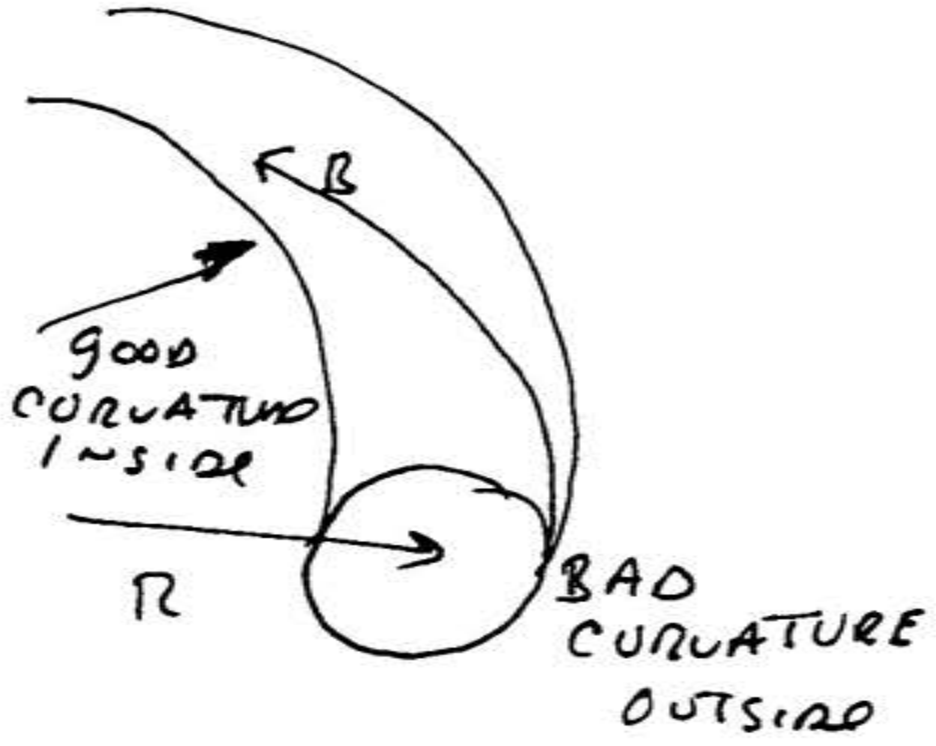

TOKAMAK
($k_\parallel \neq 0$)

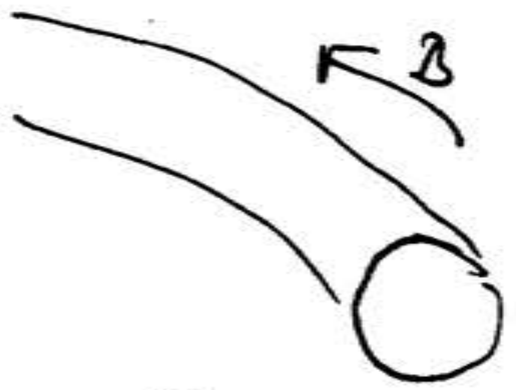

PURE TOROIDAL FIELD
$k_\parallel = 0$

WHEN $k_\parallel \neq 0$ (LIKE A TOKAMAK)

$$\nabla_\perp \cdot J_\perp = -\nabla_\parallel \cdot J_\parallel$$

$$\nabla_\perp \cdot J_{POL} + \nabla_\parallel \cdot J_\parallel + \nabla_\perp \cdot J_{CURVATURE} = 0$$

↑ FIELD LINE BENDING

$$j \frac{M_i n_0}{B^2} \nabla_\perp \omega \nabla_\perp \tilde{\Phi} - \nabla_\parallel \frac{1}{\mu_0} \nabla^2 \tilde{A}_\parallel$$

$\tilde{A}_\parallel = \frac{k_\parallel}{\omega} \tilde{\Phi}$ (SINCE $\tilde{E} = 0$)

$$-j \frac{M_i n_0}{B^2} \omega k_\perp^2 \tilde{\Phi} \left(1 - \frac{k_\parallel^2 V_A^2}{\omega^2}\right) \ldots$$

Plasma Dielectric

$$V_A^2 = \frac{B^2}{\mu_0 n_0 M_i}$$

Ballooning Stability

$$\omega^2 - k_\parallel^2 V_A^2 = -(\text{DRIVE}) \frac{k_y^2}{k^2}$$

$$\text{DRIVE} = -\frac{p'}{p} \frac{2(T_e+T_i)}{M_i R_c}$$

PRESSURE DRIVE

IF $k_\parallel$ COULD GO TO ZERO (Z-PINCH)

THEN $\omega^2 = -(\text{DRIVE})\, k_y^2/k^2$ UNSTABLE WITH (DRIVE) > 0

BUT WITH FINITE $k_\parallel$, FIELD-LINE BENDING IS STABILIZING

EXAMPLE TOKAMAK: $k_\parallel \sim \frac{1}{qR} \sim$ CONNECTION LENGTH FROM OUTSIDE TO INSIDE

UNSTABLE WHEN DRIVE $> k_\parallel^2 V_A^2 \sim V_A^2/(qR)^2$

$$\text{DRIVE} \sim \frac{2(T_e+T_i)}{M_i R_c} > \frac{V_A^2}{q^2 R^2} \Rightarrow \frac{2n(T_e+T_i)}{B^2/\mu_0} > \frac{a}{R q^2}$$

Kink Modes
(The most dangerous instabilities for current-carrying plasma.)

ION POLARIZATION — FIELD LINE BENDING — PRESSURE DRIVE

$$\nabla \cdot J = 0 = \nabla \cdot J_{pol} + \nabla_{\parallel} \cdot J_{\parallel} + \nabla \cdot J_{cur} + \nabla \cdot \left(J_0 \frac{\delta \bar{B}_{\perp}}{B_{\parallel}} \right) = 0$$

DRIFT DUE TO PERTURBED FIELD

$$\nabla \cdot \left(J_0 \frac{\partial B_{\perp}}{B_{\parallel}} \right) = \frac{\delta \bar{B}_{\perp}}{B_{\parallel}} \cdot \nabla J_{\parallel 0}$$

↑ CURRENT GRADIENT DRIVE

$$J_{\perp \delta B} \sim J_{\parallel 0} \frac{\delta \bar{B}_{\perp}}{B}$$

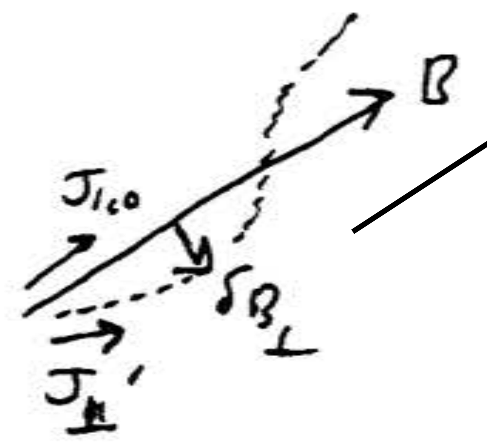

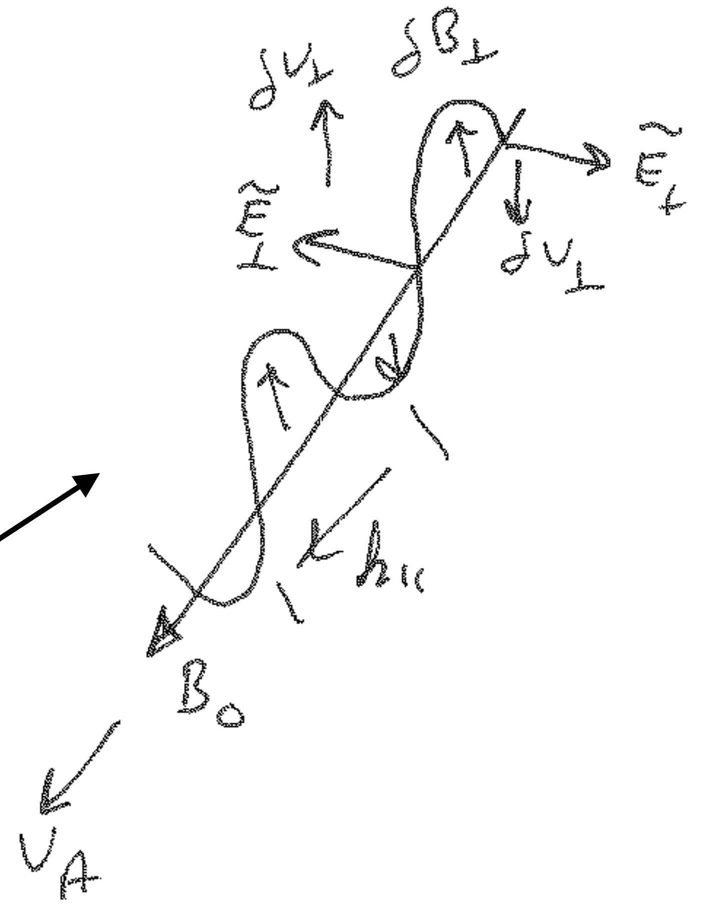

ONLY BENDING OF MAGNETIC FIELD (RELATIVELY EASY)

"ELECTROMAGNETIC DRIFT"

$$\bar{B} = B_0 \hat{z} + \delta \bar{B}_{\perp}$$

$$\hat{z} \times (\bar{v} \times \bar{B}) = \bar{v} B_{\parallel} - v_{\parallel} \bar{B} = B_{\parallel} \bar{v}_{\perp} - v_{\parallel} \delta \bar{B}_{\perp}$$

$$J_{\parallel} = J_{\parallel 0} + \tilde{J}_{\parallel}$$

$$j \hat{z} \cdot (\bar{k}_{\perp} \times \tilde{B}) = \mu_0 \tilde{J}_{\parallel} \hat{z}$$

$$\partial \tilde{B}_{\perp} = j \mu_0 \tilde{J}_{\parallel} / k_y$$

$$= j k_y \tilde{A}_{\parallel}$$

$$= -j \frac{k_{\parallel} k_y}{\omega} \tilde{\Phi}$$

$$\omega^2 - k_{\parallel}^2 V_A^2 = -(\text{DRIVE}) \frac{k_y^2}{k_{\perp}^2} + \frac{B_0}{n_0 m_i} \frac{k_{\parallel} k_y}{k_{\perp}^2} \left(\frac{dJ_{\parallel 0}}{dx} \right)$$

↑ PRESSURE DRIVE — ↑ CURRENT GRADIENT DRIVE — $\frac{dJ_{\parallel 0}}{dx} < 0$ (USUALLY)

$$k_{\parallel} = \frac{1}{qR} (m - nq)$$

SO IF $nq > m$ STABLE !!

Next: Reduced MHD

- Cylindrical Reduced MHD
- Ideal instabilities
- Tearing instabilities
- RWMs and FWMs

- M. Rosenbluth, D. Monticello, H. Strauss, and R. White, Phys Fluids 19, 1987 (1976).
- H. Strauss, D. Monticello, M. Rosenbluth, and R. White, Phys Fluids 20, 390 (1977).
- R. Izzo, et al., Phys Fluids 26, 3066 (1983).
- G.T.A. Huysmans, J.P. Goedbloed, and W. KERNER, "Free boundary resistive modes in tokamaks" Phys. Fluids B 5, 1545 (1993).

Cylindrical Reduced MHD

the order of $\epsilon^2 B_0$. To lowest order in ϵ this unknown variation of the toroidal field can be eliminated from the problem by taking the curl of the momentum equation. The resulting equations are the standard low-β tokamak reduced equations that describe free-boundary kink modes[3]:

$$R_0^2 \frac{d\nabla^2 u}{dt} = \mathbf{B}\cdot\nabla(\nabla_\perp^2 \psi),$$

$$\frac{\partial \psi}{\partial t} = R_0^2 \mathbf{B}\cdot\nabla u,$$

$$\mathbf{B} = \nabla\psi \times \nabla\zeta + I_0 \nabla\zeta,$$

$$\mathbf{V} = R_0^2 \nabla u \times \nabla\zeta,$$

$$\nabla_\perp^2 = \frac{\partial^2}{\partial R^2} + \frac{\partial^2}{\partial z^2}.$$

Here $I_0 = B_0 R_0$ and $\nabla\zeta = \hat{\zeta}/R_0$.

important

$$A_\phi = I_0(r/2)$$

$$A_\parallel \approx A_z = \psi_0(r) + \tilde{\psi}(r,\phi)$$

Plasma Physics Series

Tokamak Plasma:

A Complex Physical System

B B Kadomtsev

I V Kurchatov Institute of Atomic Energy, Moscow, Russia

Translation Editor: **Professor E W Laing**

"In memory of Boris Kadomtsev," by E P Velikhov et al 1998, *Phys.-Usp.* **41** 1155; [https://doi.org/10.1070/PU1998v041n11ABEH000508]

Institute of Physics Publishing
Bristol and Philadelphia